Journal of Applied Polymer Science

Mixed Gas and Pure Gas Transport Properties of Copolyimide Membranes

Xiao Yuan Chen, Serge Kaliaguine
Department of Chemical Engineering, Université Laval, Quebec City, Quebec, Canada G1V 0A6
Correspondence to: X. Y. Chen (E-mail: xiao-yuan.chen.1@ulaval.ca)

ABSTRACT: Copolyimides were synthesized from dianhydride of 4,4′-(hexafluoroisopropylidene)diphthalic anhydride (6FDA) with various diamine contents of 4,4′-oxydianiline (ODA) and 2,3,5,6-tetramethyl-1,4-phenylenediamine (TeMPD) by chemical imidization in a two-step procedure. Polyimides (PIs) were characterized using thermogravimetric analysis, Fourier transform infrared spectroscopy, differential scanning calorimetry, as well as specific volume and free volume. The gas transport properties for pure gas and blends of CO_2 and CH_4 for the homopolymers and 6FDA-ODA/TeMPD copolymers were investigated at 35°C and 150 psi pressure. In pure gas permeation, permeability of CO_2 and CH_4 increased with increasing TeMPD content in the diamine moiety, whereas the ideal selectivity decreased with increasing TeMPD content. In the mixed gas permeation, permeabilities and separation factor were measured as a function of CO_2 feed molar fraction for five PI membranes. The behavior of pure gas and mixed gas permeabilities and separation factor of CO_2/CH_4 mixtures as the chemical nature of the diamine and the CO_2 molar fraction in the feed gas were varied and are discussed in detail. © 2012 Wiley Periodicals, Inc. J. Appl. Polym. Sci. 000: 000–000, 2012

KEYWORDS: copolyimide; pure and mixed gas; permeability; ideal selectivity; separation factor

Received 12 January 2012; accepted 14 March 2012; published online
DOI: 10.1002/app.37728

INTRODUCTION

Natural gas will soon become an important source of energy in the world, as predicted by some of the most important energy agencies. The world consumption of natural gas has nearly tripled over the last 40 years.[1] Natural gas is not pure and must be processed before being used. The desired main component in natural gas is methane (CH_4). Other nonhydrocarbon impurities in natural gas include nitrogen, water, H_2S, and CO_2. The content of these impurities may also vary from one reservoir to another. For example, the CO_2 content may vary from a few percent up to 60% depending on the location of the natural gas well. When CO_2 is so abundant, the commercial value of natural gas is essentially null. Moreover, in the presence of water, carbonic acid may form. This can cause corrosion of transport and process equipment. This is why some of the natural gas reservoirs in Alberta, Saskatchewan, and in many other locations in the world are not exploited.[2]

There exist various technologies for the separation of hydrocarbons from nonhydrocarbon impurities, such as cryogenic distillation, adsorption, amine absorption, and membrane separation. Among these, membrane separations are particularly appealing because of their lower energy consumption and, therefore, lower costs. The applications of membrane separation for CO_2 technology are not only for CO_2 removals from natural gas but also for separation of CO_2 from enhanced oil recovery, exhaust streams and for purifying biogas.

There are several criteria for the selection of a membrane, and the most important ones are high permeability and selectivity. Compared with many membrane materials, polyimides (PIs) are highly desirable for gas separation particularly for the separation of CO_2 from CH_4. Some of them indeed exhibit high perm selectivity, high chemical resistance, thermal stability, and mechanical strength.[3,4] An upper limit for ideal selectivity of (CO_2/CH_4) in polymeric membranes versus pure CO_2 permeabilities was proposed by Robeson[5] in the early 1990s. Recently, a new corrected upper bound of CO_2/CH_4 was also reported by the same author.[6] For polymeric materials, a rather general trade-off exists between permeability and selectivity, with a corresponding "upper-bound" line.[7] In polymeric membranes application, the plasticization effect is an increase in the segmental motion of polymer chains because of the presence of one or more sorbates, in such a way that the permeability of both components increases and the selectivity decreases.[8]

LITERATURE REVIEW

Numerous researchers investigated the pure gas transport properties of homopolyimide membranes. Their results did not pass beyond the "upper bound."[9–12] Some research was also

dedicated to the gas transport properties of copolyimide and crosslinked PI membranes for pure gases. For example, 4,4′-(hexafluoroisopropylidene)diphthalic anhydride (6FDA)-1,3-phenylenediamine (TMPDA)/2,6-diamino toluene (DAT) and 6FDA-TMPDA/4,40-methylenebis(2-chloroaniline) (MOCA) copolyimides were investigated by systematically varying the diamine ratio (0/1, 0.75/0.25, 0.5/0.5, 0.25/0.75, and 1/0) by Wang et al.[13,14] Their results showed that 6FDA-based copolyimide membranes exhibit decreased pure gas permeability for CO_2 and CH_4, whereas the ideal selectivity increased with increasing DAT or MOCA content. Also, 6FDA-4,4′-oxydianiline (ODA) (4-aminophenylether) with nine different diamines : DBSA 2,4-diaminobenzenesulfonic acid, DABA 3,5-diaminobenzoicacid, DAPy 2,6-daminopyridine, DANT 1,5-diaminonaphthalene, DDS (3,3′-diaminodiphenylsulfone), MDA 4,4′-methylenedianiline, BADS 4,4′-bis(3-aminophenoxy)-diphenylsulfone, BABP 4,4′-bis(3-aminophenoxy) benzophenone, and DABN 2,6-bis(3-aminophenoxyl)benzonitrile copolyimides were prepared from one-step polymerization. The diamine monomers showed different reactivities in polycondensation and led to significant differences in molecular weight of the copolyimides. CO_2 permeability also changed with the diamine content.[15,16] 6FDA-DDS/6FAP (2,2′-bis(4-aminophenoxy)-hexafluoropropane) copolyimide was investigated by systematically varying the diamine ratio (1/0, 0.75/0.25, 0.67/0.33, 0.5/0.5, 0.33/0.67, 0.25/0.75, and 0/1). The results showed that the pure gas CO_2 permeability of these membranes increased and the ideal selectivity of CO_2/CH_4 decreased with increasing 6FAP content.[17]

Even though the majority of researchers worked with pure gases, some scientists recently also investigated the mixed gas transport properties of the polymer membranes. Copolyimide membranes derived from 6FDA-6FpDA/DABA (2 : 1) have been used to separate 50/50 CO_2/CH_4 mixed gas. These polymers were crosslinked with ethylene glycol and aluminum acetylacetonate. The results indicated that CO_2 permeability is different in the pure gas and in mixed gas at 35°C and under the same feed pressure. Mixed gas permeation results showed that there are significant decreases in the separation factor resulting from bulk flow effects and nonideal gas-phase thermodynamics for CO_2/CH_4 mixtures.[18] Copolyimides derived from 6FDA-2,4,6-trimethyl-1,3-phenylenediamine/DABA (3 : 2) crosslinked with 1,3-propanediol were used as membrane materials to separate CO_2 from CH_4. Permeabilities of CO_2 as pure gas and in mixed gas (10/90 CO_2/CH_4) were both measured at 65 psi of feed pressure and at 35°C and found to be of same value of 57.5 Barrer. The ideal selectivity was 37.1, whereas the separation factor was 44.8 under the same conditions.[19]

In the mixed gases, permeation selectivity generally changes because of sorption competition, bulk flow, nonideal thermodynamics, and plasticization.[20] For a nonplasticized polymer, it is affected by the competition for Langmuir sorption sites, and this leads to solubility coefficient changes for the various components. This means that in the CO_2/CH_4 binary mixture, the flux of CO_2 can significantly increase the total flux of CH_4 so that the flux of CO_2 will be reduced, thereby reducing the selectivity. Thus, the practical separation factor is a strong function of feed conditions: temperature, pressure, and composition.[21] The relationship between mixed gas transport properties of copolyimide membranes and feed conditions (i.e., the composition) will be systematically examined in this article. Another objective of this article is to investigate the relationship between the permeabilities and component molar ratio in a copolyimide membrane involving two different amines namely ODA and 2,3,5,6-tetramethyl-1,4-phenylenediamine (TeMPD). The reason for choosing these PIs is that 6FDA-ODA has a higher selectivity but a relatively low permeability for a specific gas pair, whereas 6FDA-TeMPD has a higher permeability with a relatively low selectivity.

BACKGROUND AND THEORY

Pure Gas Permeation

Transport in nonporous polymeric membranes is based on the so-called "solution–diffusion" concept.[22,23] Graham[24] noted that gases are capable of permeating through nonporous rubber films and that this process is related to gas dissolution and diffusion in the polymeric materials. The process of permeation comprises two stages: sorption of gas by the rubber "that must depend upon a kind of chemical affinity" and diffusion of the sorbed gas molecules.[24] There are two key characteristics of gas separation membranes, i.e., permeability and selectivity.

Permeability (P) is defined as follows:

$$P = \frac{Nl}{\Delta p} \tag{1}$$

where N is the steady-state permeation flux, $\Delta p = (p_2 - p_1)$ is the pressure difference across the membrane (p_2 is the upstream pressure and p_1 is the downstream pressure; p_2 is presumed to be higher than p_1), and l is its thickness.

The ideal selectivity is defined as a ratio of permeabilities[3]:

$$\alpha_{AB} = \frac{P_A}{P_B} \tag{2}$$

where P_A and P_B are the permeability coefficients of gases A and B, respectively. By default, the more permeable gas is taken as A, so that $\alpha_{A/B} > 1$.

Barnabeo et al.[25] reported the relationship between the permeability coefficient of the random copolymer and the volume fraction of each component in a binary copolymer for gas:

$$\mathrm{Ln}(P_{12}) = \phi_1 \mathrm{Ln}(P_1) + \phi_2 \mathrm{Ln}(P_2) \tag{3}$$

Equation (4) for ideal selectivity may be derived from eq. (3):

$$\mathrm{Ln}(\alpha_{12}) = \phi_1 \mathrm{Ln}(\alpha_{AB}) + \phi_2 \mathrm{Ln}(\alpha_{AB})_2 \tag{4}$$

and for the block copolymer,

$$P_{12} = P_1 \frac{[P_2 + 2P_1 - 2\phi_2(P_1 - P_2)]}{P_2 + 2P_1 + \phi_2(P_1 - P_2)]} \tag{5}$$

where P_{12} is the permeability coefficient of copolymer, whereas P_1 and P_2 are the permeability coefficients of polymers 1 and 2, respectively. ϕ_1 and ϕ_2 are the volume fractions of monomers 1

and 2, respectively. Equation (5) was derived from Maxwell's equation for biphasic dense polymers.

Mixed Gas Permeation

Permeation data for mixed gases in glassy polymer membranes indicate that some penetrants do not permeate entirely independently of one another. A small partial pressure of a condensable species such as CO_2 in the feed gas can significantly reduce the permeability of a given constituent relative to its permeability as a pure component[21] Therefore, the permeabilities of all penetrants are decreased by this competition for Langmuir sorption sites for nonplasticized polymers. Moreover, separation factors may also decrease because of sorption competition, bulk flow, nonideal thermodynamics, and plasticization.[19]

The permeability of component i in the mixed gas permeation can be calculated using eq. (1) and is given by eq. (6):

$$P_i = P_{\text{total}} \frac{y_i(p_2 - p_1)}{x_i p_2 - y_i p_1} \tag{6}$$

P_{total} is derived from eq. (1) for mixed gas.

When gas mixtures permeate across a membrane, the separation factor (α^*_{AB}), which is the ability of a membrane to separate a binary feed gas mixture, is defined as follows[3]:

$$\alpha^*_{AB} = (y_A/y_B)/(x_A/x_B) \tag{7}$$

where y_A and y_B are the mole fractions of the components in the permeate, and x_A and x_B are their corresponding mole fractions in the feed. Equations (1) and (7) can be combined to yield eq. (8).

$$\alpha^*_{AB} = \left(\frac{P_A}{P_B}\right)\left(\frac{p_2 x_A - p_1 y_A}{x_A}\right)\left(\frac{x_B}{p_2 x_B - p_1 y_B}\right) \tag{8}$$

Equation (8) may be further simplified as follows:

$$\alpha^*_{AB} = \alpha_{AB} \frac{p_2 - p_1\left(\frac{y_A}{x_A}\right)}{p_2 - p_1\left(\frac{y_B}{x_B}\right)} \tag{9}$$

Thus, the separation factor of a membrane depends not only on the properties of the gas–polymer system but also on process parameters such as upstream and downstream pressures and the feed composition.[23] When the upstream pressure p_2 is much greater than the downstream pressure p_1 or $p_1 = 0$, i.e., $p_2 > p_1$ (y_A/x_A) and $p_2 > p_1$ (y_B/x_B), thus eq. (9) is then simplified to:

$$\alpha^*_{AB} \approx \alpha_{AB} \tag{10}$$

EXPERIMENTAL

Materials

6FDA (mp 246°C, >99%) was provided by Chriskey Company (St. Louis, USA). ODA (mp 188–192°C, 97%) was purchased from Sigma-Aldrich (Montreal, Canada), and TeMPD (mp 152°C, 98%) was obtained from TCI America (Portland, USA) and purified by vacuum sublimation. 1-Methyl-2-pyrrolidone (NMP, bp 204°C, >99.0%) was purchased from TCI America (Lenexa, USA) and purified by vacuum distillation. Acetic anhydride (bp 138–140°C, 99.5%) and triethylamine (bp 88.1°C, ≥99.5%) were received from Sigma-Aldrich (Montreal, Canada). Chloroform ($CHCl_3$, 99.8% assay by GC analysis) was obtained from VWR international LLC (Montreal, Canada), and methanol was obtained from Fisher Scientific (Montreal, Canada).

Two-Step Synthesis of Copolyimides

All the PIs (including homopolyimides and copolyimides) were synthesized by a two-step method. In the first step, polyamic acids (PAAs) derived from equimolar amounts of solid 6FDA and diamines (ODA/TeMPD mol %: 100/0, 70/30, 50/50, 30/70, and 0/100) were prepared by solution condensation in NMP. PAA solutions were prepared at solid contents up to 20% w/v. Reaction mixtures were stirred with a mechanical stirrer in an argon atmosphere and kept at 0°C with a water–ice mixture for 15 h. In the second step, PAAs were imidized to form PIs. The cyclization was achieved by chemical imidization under argon at room temperature (RT) for 24 h through the addition of acetic anhydride (dehydrating agent) and triethylamine (catalyst). The reaction scheme of copolyimide synthesis is shown in Scheme 1. PI solution was precipitated with methanol, and the precipitate was washed several times with methanol and dried at 250°C in a vacuum oven for 24 h. Imidization was confirmed by Fourier transform infrared (FTIR)-attenuated total reflectance (ATR) analysis.

Preparation of Dense Membranes

All PI membranes were prepared by the casting method for dense films. A total of 0.5 g of PI was dissolved in 10 mL of $CHCl_3$ and the solution was filtered to remove undissolved materials and dust particles. Evaporation of the solvent was done to obtain a 10–12 wt % solution. For degassing, the PI solutions were left standing in a hood for 30 min. A nascent film was cast with the solution onto a clean glass plate using a small metal container with a cover to delay solvent evaporation from the nascent membrane for 24 h. Subsequently, the cover was removed to evaporate residual solvent for 4 h. Then, the films were placed in a vacuum oven at 230°C and each membrane was annealed for 24 h. The films were finally slowly cooled in the oven from 230°C to RT and stored in a desiccator before characterization.

Characterization

Imidization conversions from PAA to PI were observed using thermogravimetric analysis (TGA) and FTIR spectroscopy. TGA was carried out under nitrogen flow using TGA-5000IR (TA Instruments). All the PI samples were heated from 50 to 650°C at a heating rate of 10°C min^{-1}.

FTIR spectra were recorded using an FTS-60 (Bio-Rad) instrument in the range of 4000–600 cm^{-1} using either KBr pellets containing 1–5 wt % of PI or on thin polymeric films. FTIR was used to confirm the functional groups within PIs and membranes.

The glass transition temperature was determined using a differential scanning calorimeter (Perkin-Elmer DSC 7) and a thermal analysis controller (Perkin-Elmer TAC 7/DX) under a nitrogen flow at a temperature up to 500°C. The samples were heated from 100 to 500°C at a rate of 10°C min^{-1}.

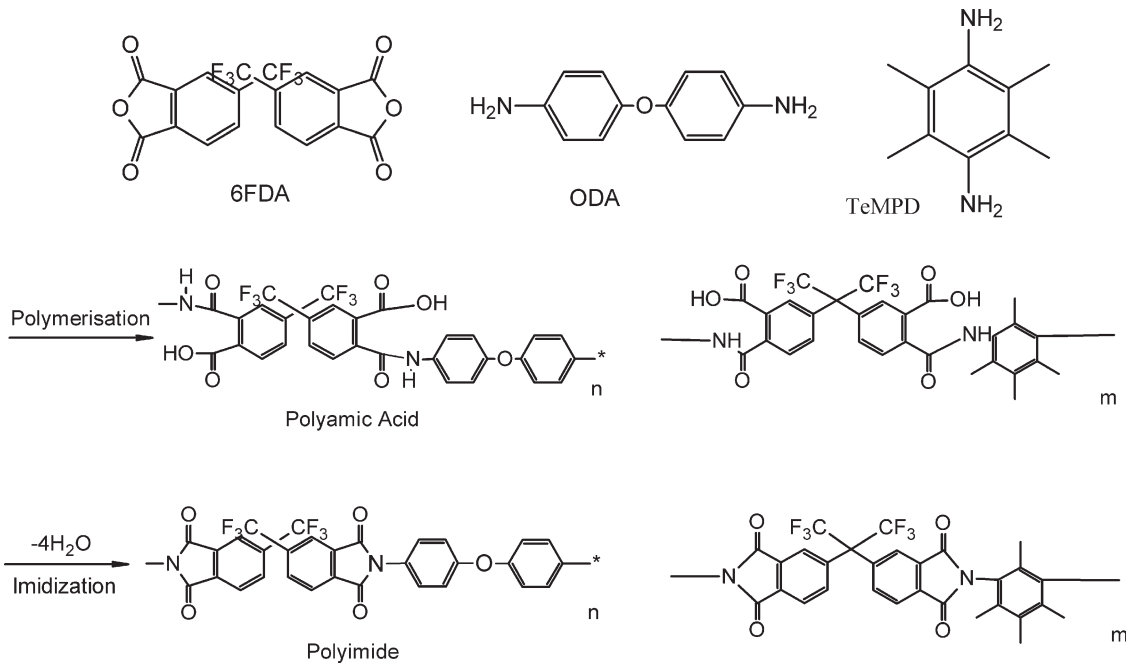

Scheme 1. Reaction scheme of copolyimides synthesis.

Young's modulus of copolyimide membranes was determined using dynamic mechanical thermal analyzer (TA Instruments, RSA-3, New Castle, DE) on samples having dimensions of about 25 × 6 × 0.02 mm^3. For tensile measurements, the extension rate was set at 1 mm min^{-1} and at 25°C.

Measurement of Transport Properties

The gas transport properties were measured by a variable pressure (constant volume) method. Figure 1 shows the apparatus for the measurement of permeability and selectivity. The membrane (A = 14.5 cm^2, 20–40 μm thickness) was mounted in a permeation cell before degassing the whole apparatus. Permeant gas was then introduced on the upstream side, and the permeant pressure on the downstream side was allowed to rise (typically from 10^{-3} to 30 Torr) until the rate of pressure increase with time became constant. It was then recorded using a pressure transducer. This steady-state condition was typically achieved after the sample had been tested for a length of time equivalent to 12 times the time lag or longer. For pure gases, the permeability coefficient, P [cm^3 (STP) cm cm^{-2} s^{-1} cm Hg^{-1}], was determined using eq. (11)[25]:

$$P = \frac{22414}{A} \times \frac{V}{RT} \times \frac{l}{\Delta p} \times \frac{dp}{dt} \tag{11}$$

where A is the membrane area (cm^2); l is the membrane thickness (cm); Δp is the upstream pressure (psi); V is the downstream volume (cm^3); R is the universal gas constant (6236.56 cm^3 cm Hg mol^{-1} K^{-1}); T is the absolute temperature (K); and dp/dt is the permeation rate (psi s^{-1}). The gas permeabilities of polymer membranes were characterized by a mean permeability coefficient with units of Barrer [1 Barrer = 10^{-10} cm^3 (STP) cm cm^{-2} s^{-1} cm Hg^{-1}].

The diffusion coefficient was calculated by the time-lag method,[26] represented by eq. (12):

$$D = \frac{l^2}{6\theta} \tag{12}$$

where θ is the time lag. Once P and D were determined, the apparent solubility coefficient S could be obtained from eq. (13).

$$P = DS \tag{13}$$

For binary CO_2/CH_4 mixed gases, the permeability coefficient and separation factor were determined using eqs. (6) and (7), respectively, introducing experimental values of gas-phase mole fractions y_i and x_i. The accepted measured values of molar

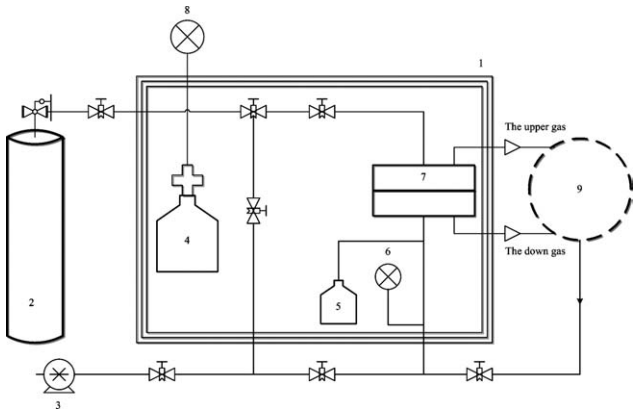

Figure 1. Permeability and selectivity measurement setup. 1: Heated chamber; 2: supply gas cylinder; 3: vacuum pump; 4: the feed reservoir volume; 5: the permeate reservoir volume; 6: pressure transducer for downstream (−15 to 15 psi); 7: membrane cell; 8: pressure gauge of upstream (0–1000 psi); and 9: 2-position and 10 ports valve and gas chromatograph.

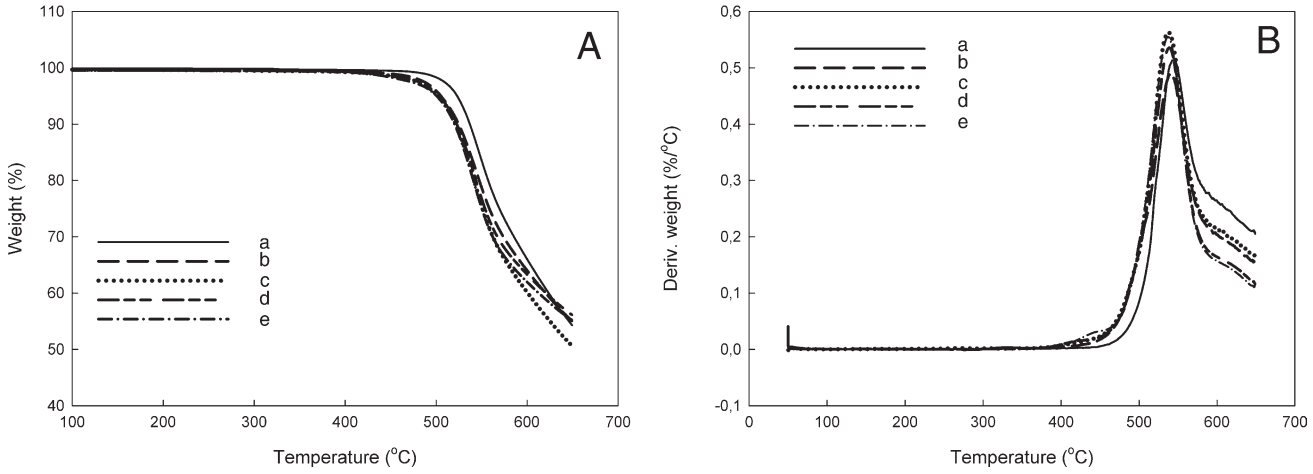

Figure 2. TGA (A) and DTG (B) analysis of copolyimides. (a) 6FDA-ODA, (b) 6FDA-ODA(70%)-TeMPD(30%), (c) 6FDA-ODA(50%)-TeMPD(50%), (d) 6FDA-ODA(30%)-TeMPD(70%), and (e) 6FDA-TeMPD.

composition were average values of at least five measurements after steady composition was reached. The relative error on these measured values was <2%. The stable composition was indeed considered reached well after the 12 times lag period.[27] It should be noted that no sweep gas was used, and that the downstream volume was evacuated and the downstream pressure was allowed to rise, ranging typically from 3 to 5 psi during the steady composition period.

RESULTS AND DISCUSSION

Polymer Membrane Characteristics

Thermal Analysis. The results of TGA and DTG are shown in Figure 2. Characteristic temperatures read from TGA curves and determined as the peak temperature in derivative thermogravimetry (DTG) plots are listed in Table I. TGA plots record the weight change of the materials when heated at a 10°C min^{-1} rate. A total of 5 and 10% weight loss temperatures are usually reported to characterize the thermal stability of a material. The derivative of the TGA curves, i.e., DTG, depicts the rate of pyrolysis. TGA and DTG curves of the PIs are exhibited in Figure 2. The $T_{d5\%}$ and $T_{d10\%}$ of the PIs demonstrate that ODA yields a higher thermal stability than TeMPD. From 25 to 400°C, all the curves were smooth, which provides proof that there was no remnant hydroxyl group and that the imidization conversion was complete. In the DTG plots of the PIs, all the curves showed one peak. The decomposition temperature was from 537 to 546°C. There was no residual solvent or hydroxyl group that would have evolved at lower temperature.

Table I. Characteristic Temperatures (°C) from TGA and DTG

Polyimide membrane	$T_{d5\%}$ wt. loss	$T_{d10\%}$ wt. loss	DTG
6FDA-ODA	522	536	546
6FDA-ODA(70%)-TeMPD(30%)	504	524	540
6FDA-ODA(50%)-TeMPD(50%)	502	522	539
6FDA-ODA(30%)-TeMPD(70%)	502	523	538
6FDA-TeMPD	500	520	537

FTIR Analysis. FTIR was used to confirm the PI groups in PAAs. As shown in Figure 3, the appearance of the absorption bands at 1727 cm^{-1} (asymmetric stretch of the carbonyl group, imide I band), 1781 cm^{-1} (symmetric stretch of the carbonyl group in the five-membered ring, imide II band), 1377 cm^{-1} (C—N stretch), 1117 cm^{-1} (imide III band), and 720 cm^{-1} (deformation of the imide ring or to the imide IV carbonyl group) confirmed the formation of imides.[28,29] A weak absorption band can be found at 3460 cm^{-1}, which may indicate the existence of primary amino group.[30] These amino groups may be the end groups of the PI chain in higher content in low molecular weight. There are no absorption bands at 3350 and 3180 cm^{-1}, 3320–3070 cm^{-1}, and 1670–1630 cm^{-1}, which would have been attributed to the amides and acids. Therefore, for the

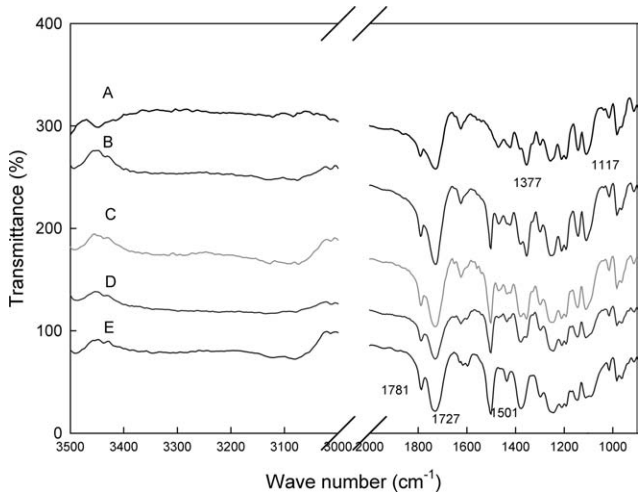

Figure 3. FTIR spectra of a series of copolyimides of 6FDA-ODA-TeMPD. (a) 6FDA-ODA, (b) 6FDA-ODA(70%)-TeMPD(30%), (c) 6FDA-ODA(50%)-TeMPD(50%), (d) 6FDA-ODA(30%)-TeMPD(70%), and (e) 6FDA-TeMPD.

Table II. Glass Transition Temperature (°C) and Mechanical Properties of 6FDA-ODA/TeMPD Copolyimides

Polymer membranes	T_g, this work	T_g, from eq. (14)	T_g, from eq. (15)	Young's modulus (GPa)	Elongation at break (%)
6FDA-ODA(100%)	294	294	294	1.82	12.4
6FDA-ODA(70%)-TeMPD(30%)	315	321	325	1.87	7.3
6FDA-ODA(50%)-TeMPD(50%)	335	344	349	1.93	5.9
6FDA-ODA(30%)-TeMPD(70%)	359	370	376	1.99	3.9
6FDA-TeMPD(100%)	420	420	420	2.10	3.8

copolyimides 6FDA-ODA-TeMPD, the imidization of PAAs was indeed complete.

Glass Transition Temperature and Mechanical Properties. Table II summarizes the experimental glass transition temperature of 6FDA-ODA/TeMPD copolyimides and those calculated by Fox equation[31] and Couchman method[30] [eqs. (14) and (15)]:

$$\frac{1}{T_g} = \frac{w_1}{T_{g1}} + \frac{w_2}{T_{g2}} \tag{14}$$

$$\ln(T_g) = w_1 \ln(T_{g1}) + w_2 \ln(T_{g2}) \tag{15}$$

where T_{g1}, T_{g2} and w_1, w_2 are the glass transition temperatures and the weight fractions of the two components, respectively. The weight fraction was defined as follows:

$$w_1 = \frac{m_1 M_1}{m_1 M_1 + m_2 M_2} \tag{16}$$

where m_1 and m_2 are the molar fraction and M_1 and M_2 are the molecular weights of the repeat units of homopolyimides 1 and 2, respectively. Here, for 6FDA-ODA and 6FDA-TeMPD, M_1 and M_2 are 606 and 572 g mol^{-1}, respectively. The T_g of homopolyimide 6FDA-TeMPD was similar to the experimental value in Refs. 32 and [33]. The T_g of 6FDA-ODA was similar to the values reported in Refs. 15 and [16]. Table II shows the comparison between experimental and predicted values. It is clear that the values calculated from Couchman method [eq. (15)] are higher than those derived from Fox equation [eq. (14)]. The experimental data are lower than the values from these two equations. They all increased with TeMPD content. This means that the interstitial spaces among chains in the molecule conformation are different and, thus, create fractional free volume (FFV), which increases with TeMPD content. The permeability increases with TeMPD content, and the permeability of copolyimide TeMPD (30%), TeMPD (50%), and TeMPD (70%) deviates from the ideal case of copolyimide (see Figure 4).

Young's modulus of copolyimide membranes was obtained from the slope of stress–strain curves at low deformation (linear elastic) and represents the rigidity of the material using dynamic mechanical analysis. Young's modulus and elongation at break of five copolyimide membranes are shown in Table II. The data showed that Young's modulus of the five PI membranes slowly increases with the addition of TeMPD. On the other hand, elongation at break decreases with increasing TeMPD content. Overall, 6FDA-TeMPD(100%) membrane is more brittle. For example, the elongation at break of 6FDA-ODA(100%) is 12.4% and the one of 6FDA-TeMPD(100%) is lower at 3.8%.

Specific Volume and Free Volume. Density, specific volume, and specific free volume of homopolyimide and copolyimides are shown in Table III. Density was determined from the weight of a membrane clipping of measured dimensions. V stands for the observed specific volume, calculated from the measured density. V_0 is the volume occupied, calculated from the van der Waals volume (V_w), and by the relation $V_0 = 1.3\ V_w$.[34] The Van

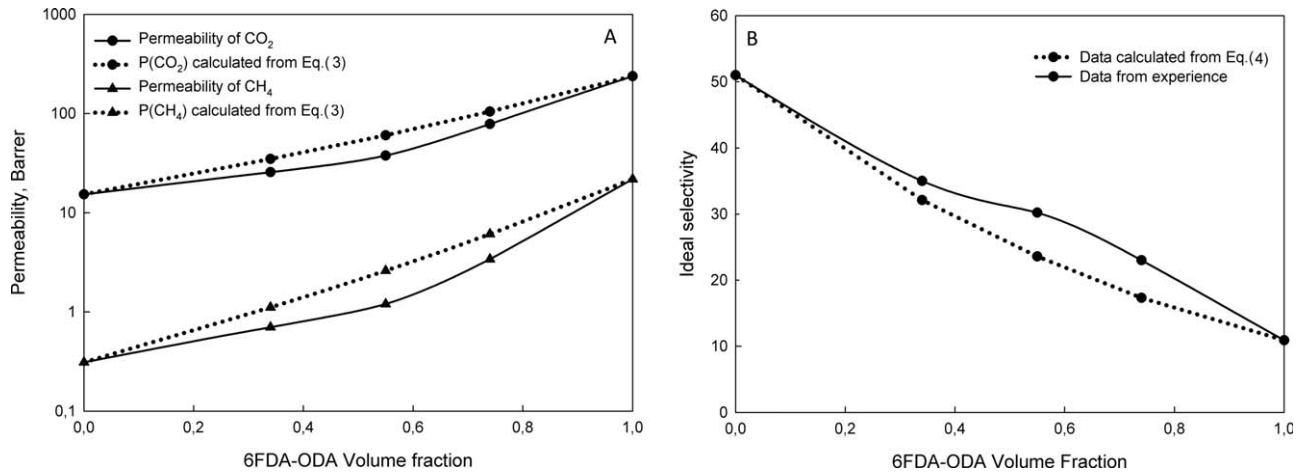

Figure 4. Gas permeability (A) and ideal selectivity (B) function of ODA diamine content.

Table III. Specific Volume and Free Volume

Polymer	ρ (g cm^f)	V (cm^3 g^{-1})	V_{ideal} (cm^3 g^{-1})	V_0 (cm^3 g^{-1})	FFV_{ideal}	FFV
6FDA-ODA(100%)	1.455	0.687	0.687	0.571	0.169	0.169
6FDA-ODA(70%)-TeMPD(30%)	1.423	0.703	0.706	0.584	0.173	0.169
6FDA-ODA(50%)-TeMPD(50%)	1.400	0.714	0.719	0.593	0.175	0.170
6FDA-ODA(30%)-TeMPD(70%)	1.370	0.730	0.732	0.602	0.177	0.176
6FDA-TeMPD(100%)	1.333	0.750	0.750	0.615	0.180	0.180

der Waals volume can be obtained from Bondi's group contribution.[34] For the copolyimide, V_w was calculated by eq. (17):

$$V_w = m_1 V_{w1} + m_2 V_{w2} \tag{17}$$

where V_{w1} and V_{w2} are the van der Waals volumes of homopolymers 1 and 2, respectively. V_{ideal} is the ideal specific volume. It was estimated by eq. (18):

$$V_{ideal} = w_1 V_1 + w_2 V_2 \tag{18}$$

The specific free volume is defined as the difference between the observed specific volume or ideal specific volume and the volume occupied. The FFV of a material is calculated using eq. (19):

$$FFV = \frac{V - V_0}{V} \tag{19}$$

The ideal FFV is obtained by eq. (20):

$$FFV_{ideal} = \frac{V_{ideal} - V_0}{V_{ideal}} \tag{20}$$

Table III shows that FFV values increase with increasing 6FDA-TeMPD content in the copolyimides. Comparing the values of FFV and FFV_{ideal}, the FFV of 6FDA-ODA(70%)-TeMPD(30%), 6FDA-ODA(50%)-TeMPD(50%), and 6FDA-ODA(30%)-TeMPD(50%) copolymer was lower than FFV_{ideal}. This would explain why the permeability of these copolyimides is lower than the calculated values (see Figure 4).

Gas Transport Properties

Permeability, Ideal Selectivity, and Separation Factor. The permeabilities of pure CO_2 and pure CH_4, ideal selectivity, and separation factor of mixed gas of 6FDA-ODA/TeMPD series copolyimide membranes measured at 35°C and 150 psi feed pressure are summarized in Table IV. The permeability data for the homopolyimide 6FDA-ODA and 6FDA-TeMPD reported in Ref. 35 were used for comparison with the data in this study. The differences between these data and our measured values may be due to different membrane preparation history especially in the case of CO_2 permeability of the 6FDA-TeMPD membrane. From Table IV, it can be seen that the pure gas permeabilities of CO_2 and CH_4 both increase with the addition of TeMPD, whereas the ideal selectivity decreases. 6FDA-ODA membrane exhibits the highest selectivity and lowest permeability of the five PI membranes studied in this work, whereas the 6FDA-TeMPD membrane shows the highest permeability and the lowest selectivity. These are caused by the methyl groups of the diamine moiety of TeMPD, connected in both ortho positions to each imide ring. The methyl substituents restrict internal rotation around the bonds between the phenyl and imide rings. The methyl groups inhibit internal rotation around the bond between the diamine moiety ring and the imide ring and both aromatic rings are perpendicular to each other.[19] The rigidity and the nonplanar structure of the polymer chain and the bulkiness of methyl groups make chain packing inefficient, resulting in increases in both diffusion and solubility coefficients of the gases (permeability) and decreases in ideal selectivity. Although the 6FDA-ODA PI membrane displays low gas permeability and high selectivity because of the mobile linkages in their diamine moieties, carbonyl and ether linkages make the packing of polymer chains more efficient, because of a high degree of conformational freedom.[35]

A comparison of permeability coefficients of the two gases obtained from experiments and calculated from eq. (3) is shown in Figure 4(A). The ideal selectivity of all copolyimides for both gases could be calculated from eq. (4), and the data from the experiments are shown in Figure 4(B). It can be seen that the permeability coefficients of the three copolyimides [6FDA-ODA(70%)-TeMPD(30%), 6FDA-ODA(50%)-TeMPD(50%), and 6FDA-ODA(30%)-TeMPD(70%)] are slightly lower and the ideal selectivities are higher than the predicted values. The results in Figure 4(A) are in agreement with the glass transition

Table IV. Permeabilities, Ideal Selectivity, and Separation Factor of CO_2/CH_4

Copolyimide membrane	P_{CO_2} (Barrer)	P_{CH_4} (Barrer)	α_{CO_2}/CH_4	$\alpha^*_{CO2/CH4}$ [a]
6FDA-ODA[b]	16.7	0.3	49	
6FDA-ODA(100%)[c]	15.3	0.3	51.0	50.8
6FDA-ODA(70%)-TeMPD(30%)	25.6	0.7	38.3	37.6
6FDA-ODA(50%)-TeMPD(50%)	37.6	1.2	30.2	30.0
6FDA-ODA(30%)-TeMPD(70%)	78.3	3.4	23.0	23.0
6FDA-TeMPD(100%)	2380	21.8	10.9	10.5
6FDA-TeMPD[b]	420	25.4	16.5	

[a]Mixed gas (50%/50% CO_2/CH_4), [b]Data from Ref. 35, [c]In molar ratio of diamines in diamine mixture.

Table V. Diffusion Coefficient and Solubility Coefficient

	D ($\times 10^{-8}$ cm^2 s^{-1})		S [cm^3 (STP) cm^{-3} cm Hg^{-1}]		Selectivity	
Copolyimide membrane	CO_2	CH_4	CO_2	CH_4	D_{CO_2}/D_{CH_4}	S_{CO_2}/S_{CH_4}
6FDA-ODA(100%)	2.10	0.24	0.078	0.013	8.8	6.00
6FDA-ODA(70%)-TeMPD(30%)	2.58	0.44	0.084	0.016	5.9	5.25
6FDA-ODA(50%)-TeMPD(50%)	3.00	0.56	0.128	0.038	5.4	3.37
6FDA-ODA(30%)-TeMPD(70%)	4.79	0.93	0.150	0.052	5.1	2.88
6FDA-TeMPD(100%)	15.30	3.46	0.200	0.074	4.4	2.70

temperature and the FFV analysis, which both show experimental values lower than the predicted ones.

For mixed CO_2/CH_4 gas, the separation factors in 50 : 50 mixtures of CO_2 and CH_4 for the five membranes are very close to the ideal selectivity (Table IV). This minor loss is due to sorption competition and possibly plasticization. According to eq. (9), the separation factor ($\alpha^*_{CO2/CH4}$) is normally smaller than the ideal selectivity ($\alpha_{CO_2/CH4}$) in gas-phase separation ($\frac{y_A}{(x_A} > \frac{y_B}{x_B)}$).

Gas Diffusivity and Solubility Coefficients of Copolyimide Membranes. According to the "solution–diffusion" concept, the gas permeation process in nonporous polymeric membranes comprises two processes: solubilization and diffusion. The experimental values of diffusion coefficients (D) of CO_2 and CH_4 for the five copolyimide membranes are shown in Table V. These coefficients were determined by the time-lag method [eq. (12)]. For example, the diffusivity of CO_2 for 6FDA-ODA(50%)-TeMPD(50%) membrane was obtained from the time lag determined as shown in Figure 5. The slope of the linear part of the $p(t)$ curve is used in eq. (11) to determine the permeability P_{CO_2}. This value is now introduced in eq. (13) to calculate the solubility (S) at 35°C and 150 psi upstream pressure. It is seen that diffusivity and solubility coefficients of CO_2 and CH_4 increase at TeMPD diamine increasing content. In general, the diffusion coefficient of a penetrant in a polymer decreases with increasing penetrant molecular size ($D_{CO_2} > D_{CH_4}$).[36] Another reason might be from differences in shape and size of the two molecules, CO_2 being more rod-like and having lower kinetic diameter (0.33 nm), whereas CH_4 is more spherical and slightly larger (0.38 nm). For solubility coefficients, CO_2 being a condensable gas has higher solubility than CH_4 in the PI.

The gas diffusion coefficient and diffusivity selectivity for glassy polymers are determined by the packing density and local mobility of polymer chains.[37,38] The packing density of polymer chains is considered to reflect the FFV and size distribution of free volume holes. The PIs derived from diamines TeMPD display very high D values, which are attributed to the difference in size distribution of free volume holes between 6FDA-ODA and 6FDA-TeMPD. Such variation has been demonstrated by positron annihilation lifetime spectroscopy of 6FDA-ODA and 6FDA-TeMPD in Ref. 39.

Table V shows that the solubility coefficients of both CO_2 and CH_4 in copolyimides increase with increasing diamine TeMPD content, likely because of a higher free volume and particular size distribution of volume holes in the FDA-TeMPD PI. The selectivities of diffusivity and solubility coefficients both decrease with increasing diamine TeMPD content.

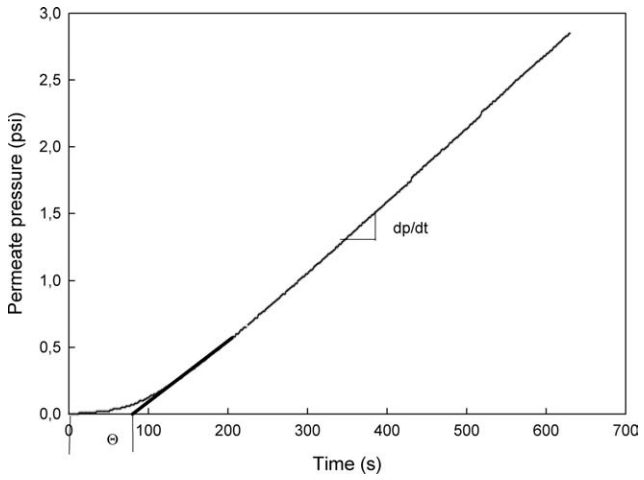

Figure 5. Typical permeation and time-lag curve for the permeation of CO_2 in the 6FDA-ODA(50%)-TeMPD(50%) membrane.

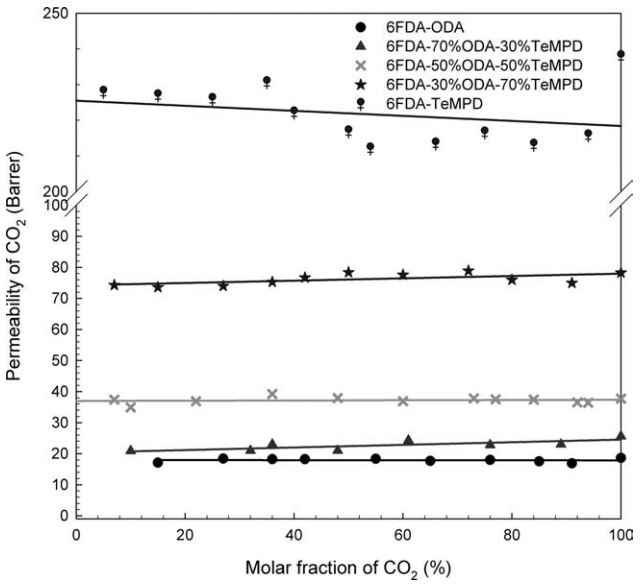

Figure 6. Permeability of CO_2 in CO_2/CH_4 mixed gas as a function of CO_2 molar fraction.

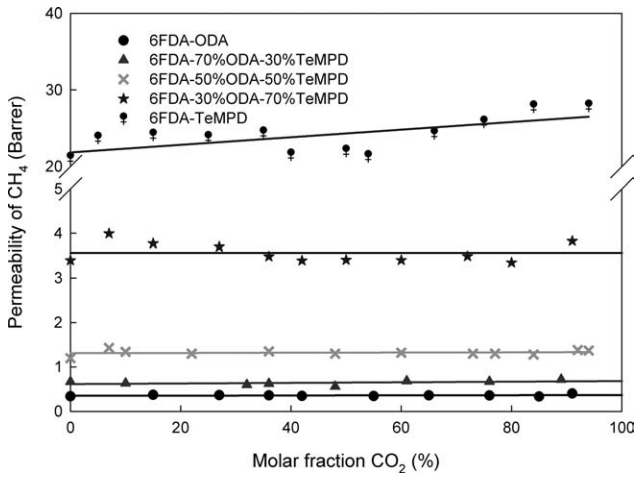

Figure 7. Permeability of CH_4 in CO_2/CH_4 mixed gas as a function of CO_2 molar fraction.

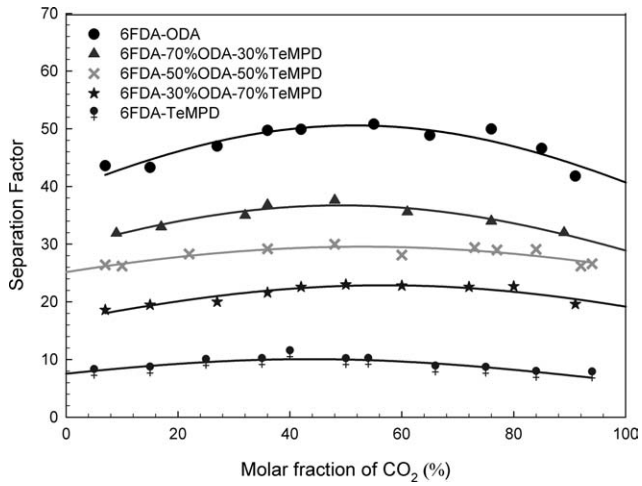

Figure 8. Separation factor in CO_2/CH_4 mixed gas as a function of CO_2 feed concentration (molar fraction).

Permeability of CO_2 in CO_2/CH_4 Mixed Gas. Figure 6 shows the measured values of CO_2 permeability in CO_2/CH_4 mixed gas as a function of CO_2 feed concentration (molar fraction) at 35°C and 150 psi for the five copolyimide membranes examined in this study. It was found in Figure 6 that the permeability of CO_2 in mixed gas is smaller than that in pure gas. The observed reduction in permeability is most likely due to the competition between the penetrants for Langmuir sorption sites in a glassy polymer, as the permeation follows the solution–diffusion mechanism.[40] In these binary mixtures, the presence of CH_4 is believed to reduce the solubility coefficient of CO_2 by competition in occupying the unrelaxed volume. Hence, CO_2 permeability is lowered by the presence of CH_4. There is a tendency for permeability to increase with increasing TeMPD content in mixed gas as well as in the pure gas. The permeability of CO_2 stays almost constant with increasing CO_2 feed concentration in the mixed gas system.

Permeability of CH_4 in CO_2/CH_4 Mixed Gas. The measured permeabilities of CH_4 in CO_2/CH_4 mixed gas as a function of CO_2 mole fraction at 35°C and 150 psi for the five copolyimide membranes are shown in Figure 7. The results indicate that the permeability of CH_4 also increases with increasing TeMPD content in mixed gas just like in the pure gas. It was found that permeability of CH_4 in mixed gas is higher than in the pure gas and thus that the presence of CO_2 increases CH_4 permeability. The presence of CO_2 will eventually lead to plasticization and increased free volume, chains mobility, and interstitial space among chains. The permeability of CH_4 is almost constant with increasing CO_2 mole fraction.

Separation Factor. The separation factors calculated using eq. (7) for gas blends are lower than for neat gases. A similar behavior was reported in the literature.[41,42] The separation factors of the five membranes show similar trends as a function of CO_2 mole fraction in the feed (Figure 8). At CO_2 mole fraction lower than about 50%, the separation factor increased with CO_2 mole fraction, whereas above this value these factors decreased. Such a result was also obtained in our earlier work.[43] It was in contradiction with the results obtained by Basu et al. who found that the separation factor (α^*) decreased continuously with CO_2 mole fraction for their asymmetric PI membranes (Matrimid, polysulfone, and blend of these two polymers).[44] These effects are illustrated in Figure 9 where the mixed gas separation factors are plotted as functions of CO_2 permeabilities in the mixed gas. For sake of clarity, the values of ideal selectivities are also reported as a function of pure CO_2 permeation. It may be observed that the maximum separation factors are very close to the ideal selectivity. The variation in separation factor is similar to those of ideal selectivity. The correlation between these two factors justifies to some extent, the common practice of describing selectivities by only reporting separation factors.

CONCLUSIONS

In this work, a systematic study of copolyimide membrane composition on pure and CO_2/CH_4 mixed gas permeability and separation properties was performed.

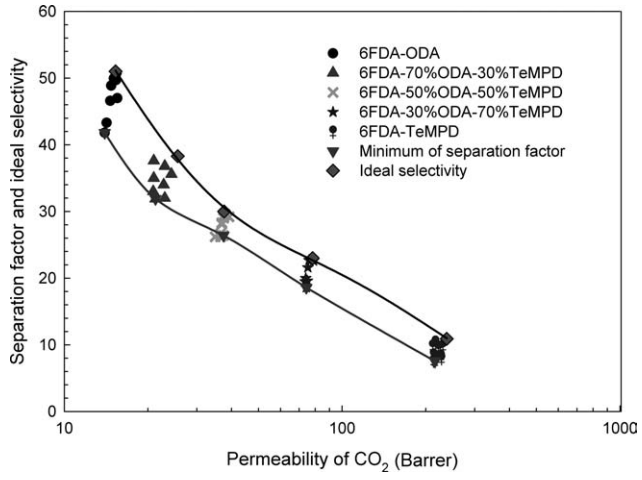

Figure 9. Separation factors of mixed gas and ideal selectivity as a function of CO_2 permeability.

The objective of this study was to illustrate how known correlations[25] could represent experimental permeability and separation factor values as functions of copolyimide composition. Figure 4(A,B) allows establishing that these correlations were not very precise when both diamine components were in comparable concentrations in the membrane.

In addition, the work provided a clear diagram (Figure 9) indicating how actual separation factors were related to ideal selectivities over the whole range of copolyimide membrane composition.

A complete analysis of the effect of copolyimide composition on CO_2 and CH_4 diffusivity and solubility coefficient was also reported and discussed.

ACKNOWLEDGMENTS

The authors would like to thank the Natural Science and Engineering Research Council of Canada (NSERC) for financial support through a strategic grant. X. Y. Chen thanks Fonds QuÕbÕcois de Recherche sur la Nature et les Technologies for a scholarship. The authors also thank Professor Denis Rodrigue for fine suggestions.

REFERENCES

1. Natural Gas Market. Available at: http://en.wikipedia.org/wiki/Natural_gas. Accessed May 4, **2010.**
2. Oil tracers LLC. Available at: http: //www.gaschem.com/evalu.html. Accessed May 1, **2010.**
3. Ghosal, K.; Freeman, B. D. *Polym. Adv. Technol.* **1994,** *5*, 673.
4. Freeman, B. D.; Pinnau, I. Polymer Membrane for Gas and Vapor Separations: Chemistry and Material Science; American Chemical Society: Washington, DC, **1999.**
5. Robeson, L. M. *J. Membr. Sci.* **1991,** *62*, 165.
6. Robeson, L. M. *J. Membr. Sci.* **2008,** *320*, 390.
7. Takekoshi, T. Polyimides: Fundamental and Applications; Malay K. Ghosh and K. L. Mittal Edts, Marcel Dekker, Inc., New York, **1996;** p 19.
8. Koros, W. J.; Hellums, M. W. "Transport properties" Encyclopedia of Polymer Science 2nd Edition, Ed. by J. I. Kroschwitz, Wiley-Interscience Publishers, New York, **1989**; Supplement Volume; p 724.
9. Teplyakov, V.; Meares, P. *Gas. Sep. Purif.* **1990,** *4*, 66.
10. Okamoto, K.; Tanaka, K.; Kita, H.; Ishida, M.; Kakimoto, M.; Imai, Y. *Polym. J.* **1992,** *24*, 451.
11. Okamoto, K. I.; Tanaka, K.; Kita, H.; Nakamura, A.; Kusuki, Y. *J. Polym. Sci. Part B: Polym. Phys.* **1989,** *27*, 2621.
12. Tanaka, K.; Kita, H.; Okamoto, K. *Kobunshi Ronbunshu* **1990,** *47*, 945.
13. Wang, L.; Cao, Y. M.; Zhou, M. Q.; Liu, Q. H.; Ding, X. L.; Yuan, Q. A. *Eur. Polym. J.* **2008,** *44*, 225.
14. Wang, L.; Cao, Y. M.; Zhou, M. Q.; Zhou, S. J.; Yuan, Q. *J. Membr. Sci.* **2007,** *305*, 338.
15. Xiao, S. D.; Huang, R. Y. M.; Feng, X. S. *Polym. Eng. Sci.* **2008,** *48*, 795.
16. Xiao, S. D.; Huang, R. Y. M.; Feng, X. S. *Polymer* **2007,** *48*, 5355.
17. Mikawa, M.; Nagaoka, S.; Kawakami, H. *J. Membr. Sci.* **1999,** *163*, 167.
18. Wind, J. D.; Staudt-Bickel, C.; Paul, D. R.; Koros, W. J. *Ind. Eng. Chem. Res.* **2002,** *41*, 6139.
19. Hillock, A. M. W.; Koros, W. J. *Macromolecules* **2007,** *40*, 583.
20. Kamaruddin, H. D.; Koros, W. J. *J. Membr. Sci.* **1997,** *135*, 147.
21. Koros, W. J.; Chern, R. T.; Stannett, V.; Hopfenberg, H. B. *J. Polym. Sci. Polym. Phys. Ed.* **1981,** *19*, 1513.
22. Paul, D. R. *Sep. Purif. Method* **1976,** *5*, 33.
23. Wijmans, J. G.; Baker, R. W. *J. Membr. Sci.* **1995,** *107*, 1.
24. Graham, T. *J. Membr. Sci.* **1866,** *100*, 27.
25. Barnabeo, A. E.; Creasy, W. S.; Robeson, L. M. *J. Polym. Sci. Polym. Chem. Ed.* **1975,** *13*, 1979.
26. Barrer, R. M.Diffusion in and Through Solids;Cambridge University Press, London, UK, **1951; p 18.**
27. O'Brien, K. C.; Koros, W. J.; Barbari, T. A.; Sanders, E. S. *J. Membr. Sci.* **1986,** *29*, 229.
28. Pramoda, K. P.; Liu, S. L.; Chung, T. S. *Macromol. Mater. Eng.* **2002,** *287*, 931.
29. Sroog, C. E.; Endrey, A. L.; Abramo, S. V.; Berr, C. E.; Edwards, W. M.; Olivier, K. L. *J. Polym. Sci. Part A: Gen. Pap.* **1965,** *3*, 1373.
30. Couchman, P. R. *Macromolecules* **1978,** *11*, 1156.
31. Fox, T. G. *Bull. Am. Phys. Soc.* **1956,** *1*, 123.
32. Lin, W. H.; Vora, R. H.; Chung, T. S. *J. Polym. Sci. Part B: Polym. Phys.* **2000,** *38*, 2703.
33. Tanaka, K.; Okano, M.; Toshino, H.; Kita, H.; Okamoto, K. I. *J. Polym. Sci. Part B: Polym. Phys.* **1992,** *30*, 907.
34. Bondi, A. *J. Phys. Chem.* **1964,** *68*, 441.
35. Yampolskii, Y.; Pinnau, I.; Freeman, B. D. Materials Science of Membranes for Gas and Vapor Separation; John Wiley & Sons, Ltd., West Sussex, England, 2006; p 293.
36. Berens, A. R.; Hopfenberg, H. B. *J. Membr. Sci.* **1982,** *10*, 283.
37. Kim, T. H.; Koros, W. J.; Husk, G. R.; Obrien, K. C. *J. Membr. Sci.* **1988,** *37*, 45.
38. Stern, S. A.; Mi, Y.; Yamamoto, H.; Stclair, A. K. *J. Polym. Sci. Part B: Polym. Phys.* **1989,** *27*, 1887.
39. Tanaka, K.; Kawai, T.; Kita, H.; Okamoto, K.-i.; Ito, Y. *Macromolecules* **2000,** *33*, 5513.
40. Coker, D. T.; Freeman, B. D.; Fleming, G. K. *AIChE J.* **1998,** *44*, 1289.
41. Wang, R.; Cao, C.; Chung, T. S. *J. Membr. Sci.* **2002,** *198*, 259.
42. Raymond, P. C.; Koros, W. J.; Paul, D. R. *J. Membr. Sci.* **1993,** *77*, 49.
43. Chen, X. Y.; Rodrigue, D.; Kaliaguine, S. *Sep. Purif. Technol.* **2012,** *86*, 221.
44. Basu, S.; Cano-Odena, A.; Vankelecom, I. F. *J. Sep. Purif. Technol.* **2010,** *75*, 15.